

Motorcycle Emission Simulation Using AVL Cruise M Software

Pham Huu Tuyen¹, Nguyen Cao Cuong^{1,2*}

¹School of Mechanical Engineering, Hanoi University of Science and Technology, Ha Noi, Vietnam

²Hanoi Vocational College of Technology, Ha Noi, Vietnam

*Corresponding author email: cuongnc@hactech.edu.vn

Abstract

The study utilizes AVL Cruise M software to simulate emissions and fuel consumption from the Honda Future 125 Fi motorcycle, a popular model in Vietnam. Simulations were conducted under three standard driving cycles: World Motorcycle Test Cycle (WMTC), European Motorcycle Driving Cycle (ECE R40), and Hanoi Motorcycle Driving Cycle (HMDC) aiming to assess CO, HC and NOx emissions under different operational conditions. The results demonstrate that each driving cycle has a distinct impact on emission levels, with significant differences in CO, HC, and NOx concentrations across the cycles. The HMDC cycle, which reflects typical traffic conditions in Vietnam, is identified as a suitable choice for simulating motorcycle emissions in urban areas. These findings provide an additional tool for calculating motorcycle emissions, supporting the development of more effective air pollution control strategies in the future.

Keywords: Emission simulation, motorcycle emissions, AVL Cruise M, driving cycle.

1. Introduction

Air pollution is one of the main factors affecting human health and the environment [1]. According to the World Health Organization, road transport is a major contributor to air pollution in urban areas, causing approximately 9 million premature deaths in 2022, primarily due to exposure to PM10 and PM2.5 [2]. In Vietnam, motorcycles are the predominant mode of transportation, with over 72 million registered motorcycles, according to data from the Vietnam Register. By the end of December 2023, there were 6,545,317 and 7,800,000 motorcycles in operation in Hanoi and Ho Chi Minh City, respectively, accounting for 86% of the total vehicles on the road. Emission inventory data from 2021 to 2023 indicates that motorcycles in Hanoi emit nearly 4.6 million tons of CO₂ annually [3]. The level of emissions from motorcycles depends on various factors, such as fuel type, emission control technology, and operating conditions [5]. Accurately estimating emissions is a major challenge and requires careful consideration of various factors, including the choice of measurement methods and the scale of emission models [4].

The amount of emissions emitted depends on a number of factors, such as fuel used, emission control technology as well as operating conditions of the vehicle (driving style, cold start or hot start conditions...) [5]. Vehicle emission models are used to estimate emissions from road transport as well as to estimate emissions based on various input data. These data are distinguished according to the scale of the

model used [6]. Input data can be detailed vehicle data, such as engine specifications, driving conditions and fuel properties [7]. With sufficient input data, simulation software allows us to provide valuable information on vehicle emission levels useful for air pollution control [8]. Estimating emissions by simulation is much cheaper and more convenient as compared to that by carrying out experiment on test bench [9]. Therefore, to perform calculations under different traffic conditions and reduce testing costs, it is necessary to study and apply emission simulation software for road vehicles in general and motorcycles in particular. In the world, the use of emission simulation software has been used but the main application is cars [10]. In addition, with new types of vehicles using many emission reduction technologies, emission calculation methods also need to be supplemented and updated regularly. In Vietnam, there have been some studies on building typical driving cycles and determining emission coefficients for vehicles [11-13]. However, studies on using emission calculation methods using simulation software are rarely used and updated, especially for motorcycles due to the large number of vehicles in circulation. This paper presents a study on the application of AVL Cruise M software to simulate emissions from the popular Honda Future 125 Fi motorcycle in Vietnam. The simulations were conducted under three different standard driving cycles World Motorcycle Test Cycle (WMTC), European Motorcycle Driving Cycle (ECE R40) and Hanoi Motorcycle Driving Cycle (HMDC).

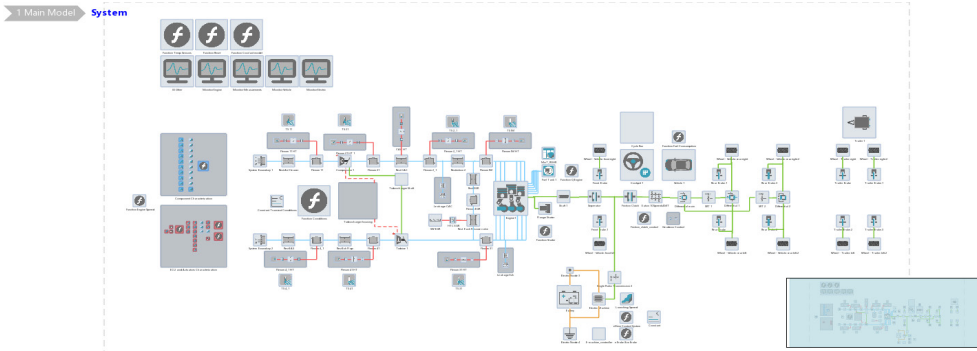


Fig. 1. Arrangement and connection of elements of electronic fuel injection engine model

2. Models in AVL Cruise M

2.1. Simulation Process

The simulation model in AVL Cruise M can be built by selecting, arranging and linking elements on the interface. To ensure accuracy, the software allows only suitable elements to be connected together. These elements are shown in Fig. 1.

The simulation process in this software with the object of transportation includes important steps as shown in Fig. 2.

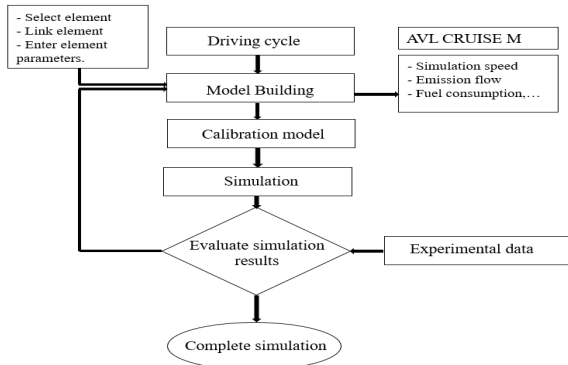


Fig. 2. Simulation process in AVL CRUISE M

2.2. Modeling Drag Forces Acting on the Vehicle

The drag force acting on the vehicle is the main parameters that determine the fuel consumption and emissions of the vehicle. Therefore, it is necessary to study and model the characteristics of the external forces acting on the vehicle. Fig. 3 illustrates the drag forces acting on the vehicle when moving.

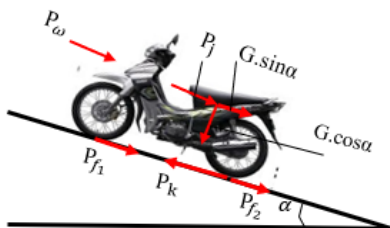


Fig. 3. Resistance force acting on the vehicle when moving

Vehicle movement can be reduced to the following types of forces: Rolling resistance, uphill resistance, aerodynamic drag and inertia resistance. The total resistance force (P_k) when the vehicle is moving is calculated according to the following formula [14]:

$$P_k = P_f \pm P_i + P_w \pm P_j \quad (1)$$

where P_k is traction force generated at the driving wheel, P_f is rolling resistance, P_i is climbing resistance or downgrade force, P_w is aerodynamic drag, P_j is inertial resistance when the vehicle moves unsteadily.

$$P_f = f \cdot G \cdot \cos \alpha \quad (2)$$

where f is coefficient of rolling resistance, G is weight of the vehicle, α is gradient angle.

The resistance of a vehicle going uphill or downhill is calculated as follows:

$$P_i = G \cdot \sin \alpha \quad (3)$$

Aerodynamic drag depends a lot on the speed of the vehicle. Aerodynamic drag can be calculated as follows:

$$P_w = W \cdot v^2 \quad (4)$$

where W is air resistance factor, v is vehicle speed.

Inertial resistance depends on the mass and acceleration of the vehicle. Inertial resistance is calculated by the following formula:

$$P_j = \frac{G}{g} \cdot j \quad (5)$$

where g is gravitational acceleration, j is acceleration of the vehicle.

2.3. Emission Models

The emission components in the AVL Cruise M software are formed according to the following modes:

2.3.1. NOx formation model

The NOx formation process is described through the following six chemical reactions in Table 1 [14].

Table 1. Chemical reactions of NO_x formation

	Stoichiometry	Rate $K_i = k_{0,i} \cdot T^a \cdot e^{\frac{TA_i}{T}}$	K_0 [cm ³ ,mol,s]	A [-]	T _A [K]
R ₁	N ₂ +O=NO+N	$r_1 = k_1 \cdot c_{N_2} \cdot c_O$	4.93E13	0.0472	38048.01
R ₂	O ₂ +N=NO+N	$r_2 = k_2 \cdot c_{O_2} \cdot c_N$	1.48E08	1.5	2859.01
R ₃	N+OH=NO+H	$r_3 = k_3 \cdot c_{OH} \cdot c_N$	4.22E13	0.0	0.0
R ₄	N ₂ O+O=NO+NO	$r_4 = k_4 \cdot c_{N_2O} \cdot c_O$	4.58E13	0.0	12130.6
R ₅	O ₂ +N ₂ =N ₂ O+O	$r_5 = k_5 \cdot c_{O_2} \cdot c_{N_2}$	2.25E10	0.825	50569.7
R ₆	OH+N ₂ =N ₂ O+H	$r_6 = k_1 \cdot c_{OH} \cdot c_{N_2}$	9.14E07	1.148	36190.66

All reaction rates r_i have units of [mol/cm³s], concentration c_i is the molar concentration at equilibrium conditions with units of [mol/cm³]. The N₂O concentration is calculated according as follows:

$$c_{N_2O} = 1.1802 \cdot 10^{-6} \cdot e^{\left(\frac{9471.6}{T}\right)} \cdot c_{N_2} \cdot \sqrt{p_{O_2}} \quad (6)$$

where c_{N_2O} and c_{N_2} are concentrations of N₂O and N₂, T is local combustion temperature, in the two zone model T is the temperature of the burned zone, p_{O_2} is partial pressure of oxygen in the gas phase.

The NO formation rate in [mol/cm³s] is calculated as follows:

$$r_{NO} = C_{PostProMult} \cdot C_{KineticMult} \cdot 2 \cdot \left(1 - \alpha^2\right) \cdot \frac{r_1}{1 + \alpha \cdot AK_2} \cdot \frac{r_4}{1 + AK_4} \quad (7)$$

with:

$$\alpha = \frac{c_{NO,act}}{c_{NO,eq}} \cdot \frac{1}{C_{PostProMult}};$$

$$AK_2 = \frac{r_1}{r_2 + r_3}; \quad AK_4 = \frac{r_4}{r_5 + r_6}$$

In this calculateure $C_{PostProMult}$ is tuning parameter to influence the rate of NO production, $C_{KineticMult}$ is tuning parameter to influence the rate of NO formation depending on distance from equilibrium conditions, α is fraction of NO, AK_i is arrhenius constants of the i^{th} reaction.

2.3.2. CO formation model

The CO emission model is based on two chemical reactions in Table 2 [15].

Table 2. Chemical reactions for CO formation

	Stoichiometry	Rate
R ₁	CO + OH = CO ₂ + H	$r_1 = 6.76 \cdot 10^{10} \cdot e^{\frac{T}{1102.0}} \cdot c_{CO} \cdot c_{OH}$
R ₂	CO + O ₂ = CO ₂ + O	$r_2 = 2.51 \cdot 10^{12} \cdot e^{\frac{-24055.0}{T}} \cdot c_{CO} \cdot c_{O_2}$

The rate of CO formation/decomposition [mol/cm³s] is calculated as follows:

$$r_{CO} = C_C \cdot (r_1 + r_2) \cdot (1 - \alpha) \quad (8)$$

where r_{CO} is rate of CO production/destruction, C_C is tuning parameter to scale the rate of CO formation, r_1 is reaction rate R_1 of CO formation, r_2 is reaction rate R_2 of CO formation, α is fraction of the actual CO concentration to its equilibrium concentration.

2.3.3. HC formation model

HC emissions are formed due to incomplete combustion, wall effect and from the lubricating oil layer on the cylinder surface evaporating and mixing with the exhaust gas [16], that include:

- *Crevice mechanism*: the amount of unburned fuel in the crevices is equal to:

$$m_c = \frac{p \cdot V_c \cdot M}{R \cdot T_p} \quad (9)$$

where m_c is mass of unburned charge in the crevices [kg], p is cylinder pressure [Pa], V_c is total crevice volume [m³], M is unburned molecular weight [kg/kmol], R is gas constant [J/(kmol K)], T_p is piston temperature [K]

- *HC absorption/desorption mechanism*: the radial distribution of the fuel mass fraction in the oil film can be determined by solving the diffusion equation:

$$\frac{\partial \omega_F}{\partial t} - D \frac{\partial^2 \omega_F}{\partial r^2} = 0 \quad (10)$$

where ω_F is mass fraction of fuel in oil film [-], t is time [s], r is radial position in oil film [m], D is relative diffusion coefficient of fuel oil [m²/s]. The diffusion coefficient can be computed by applying the following relation:

$$D = 7.4 \cdot 10^{-8} \cdot M^{0.5} \cdot T \cdot v_f^{-0.6} \cdot \mu^{-1} \quad (11)$$

where M is oil molecular weight [g/mol], T is oil temperature [K], v_f is molar volume of the fuel at normal boiling conditions [cm³/mol], μ is oil viscosity [centipoise].

- *Partial burn effects*: the unburned fuel F_{prob} is calculated by the formula below [17]:

$$F_{\text{prob}} = P \cdot C_1 \cdot e^{\frac{v_{\text{EVO}} - v_{90}}{C_2 \cdot (v_{90} - v_0)}} \quad (12)$$

$$C_1 = 0.0032 + \frac{\varphi - 1}{22} \quad \text{if } \varphi < 1$$

$$C_1 = 0.003 + ((\varphi - 1) \cdot 1.1)^4 \quad \text{if } \varphi > 1$$

$$C_2 = 0.35$$

where P is tunable parameter [-], φ is equivalence ratio [-], v_0 is 0% mass fuel burned timing [degCA], v_{90} is 90% mass fuel burned timing [degCA], v_{EVO} is exhaust valve open timing [degCA].

- *HC post oxidation*: amount of HC generated after oxidation is calculated by the Arrhenius equation [17]:

$$\frac{dC_{\text{HC}}}{dt} = -F_{\text{Ox}} \cdot f \cdot A_{\text{Ox}} \cdot \exp\left(\frac{-T_{\text{Ox}}}{T}\right) \cdot C_{\text{O}_2} \cdot C_{\text{HC}} \quad (13)$$

where C is concentration of HC and O_2 [kmole/m³], F_{Ox} is HC postoxidation multiplier [-], f is HC postoxidation scaling factor [-], T_{Ox} is activation temperature default = 18790.0 [K], A_{Ox} is frequency factor default equal to 7.7E12 [m³/kmole/s].

Below, the author presents detailed research on the application of AVL Cruise M software to simulate and calculate motorcycle emissions according to three driving cycles: WMTC, ECE R40 and HMDC.

3. Research on Building Simulation Models

3.1. Motorcycle Simulated

A Honda Future 125 Fi motorcycle popular used in Viet Nam is selected to simulate. Specification of this motorcycle is shown in Table 3.

Table 3. Specification of Honda Future 125 Fi motorcycle

Parameters	Value
Cylinder diameter and piston stroke	52.4 mm x 57.913 mm
Compression ratio	9.3:1
Maximum power/speed	6.83 kW/7500 rpm
Maximum torque/speed	10.2 Nm/5500 rpm
Fuel system	Electronic fuel injection
Gear box	Manual

3.2. Model Building

The model is built by appropriate elements such as engine, mechanical gearbox, wheel,... and input

data involved as shown in Fig. 4. The definition of the environment includes temperature, pressure, air composition,... For engine element, the Woschni model and fractal combustion model are used to calculate heat transfer coefficient and combustion process inside cylinder. The engine torque and speed are calculated and transmitted to the wheel to simulate the required driving cycle.

Driving cycles are defined by speed pattern, gear shifting behavior and cycle duration. In this study, three driving cycles including WMTC as in Fig. 5, ECE R40 and HMDC cycles are established to simulate operation condition of the motorcycle model. Table 4 summaries main parameters for these cycles.

Some elements require input signals to function properly. This is done by means of data bus connections that transmit signals between the output and input data ports. The Honda Future 125 Fi model is connected by data bus according to the channels described in Fig. 6.

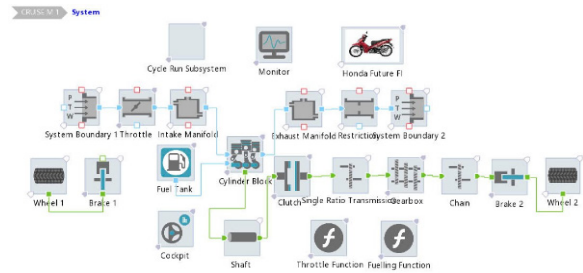


Fig. 4. Honda Future 125 Fi model

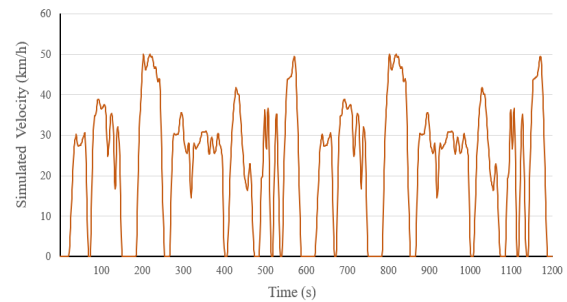


Fig. 5. WMTC driving cycle

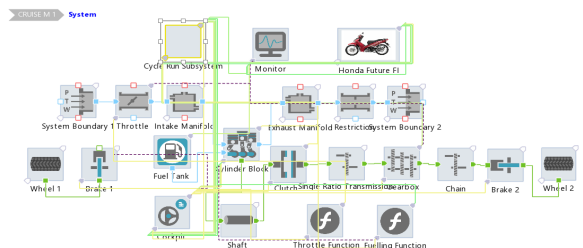


Fig. 6. Data Bus connection of Honda Future 125 Fi model elements

Table 4. Main parameters for WMTC, ECE R40 and HMDC cycles

Characteristics	Unit	WMTC	ECE R40	HMDC
Distance	km	7.59	5.97	7.07
Total time	s	1200	1200	1250
Idle (standing) time	s	234	378	136
Average speed (incl. stops)	km/h	24.4	18.4	20.4
Average driving speed (excl. stops)	km/h	28.92	23.87	27.1
Maximum speed	km/h	59.99	50.07	39.41
Average acceleration	m/s ²	0.68	0.64	0.40
Maximum acceleration	m/s ²	2.51	1.04	0.78

4. Simulation Results

Velocity, emissions and other working parameters of the motorcycle versus time can be displayed online as shown in Fig. 7.

The motorcycle model is run with WMTC driving cycle. The simulation results of the vehicle speed closely follow the required driving cycle as in Fig. 8, the error of the simulated speed and the required speed is 2%.

The simulated emissions of CO, HC, and NO_x under the WMTC cycle were compared with experimental results obtained from motorcycle testing on a dynamometer. Figs. 9 to 11 illustrate the time-based emission variations, showing that the simulation trends align closely with the measured data. The cycle-averaged values are compared in Table 5, with the highest error being 2.57% for HC emissions. This demonstrates that the model can accurately replicate emission characteristics, providing a reliable foundation for application to other driving cycles.

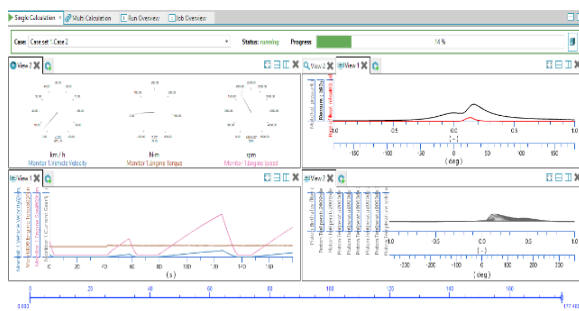


Fig. 7. Instantaneous results during simulation

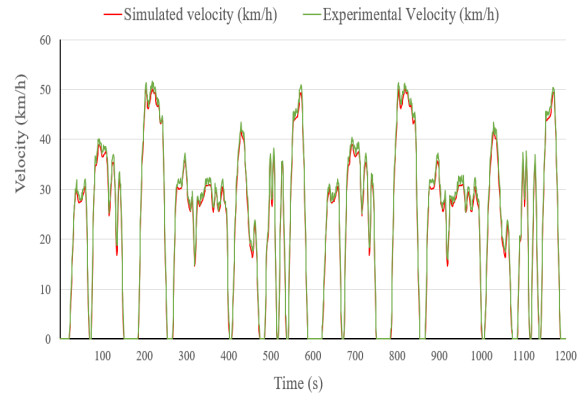


Fig. 8. Velocity according to WMTC

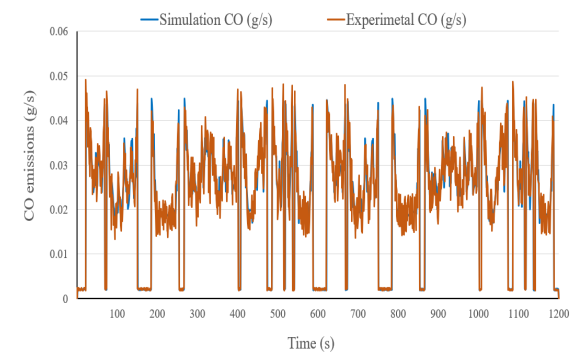


Fig. 9. CO emissions with WMTC cycle

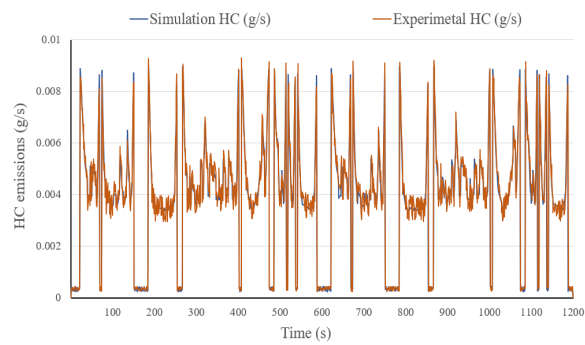


Fig. 10. HC emissions with WMTC cycle

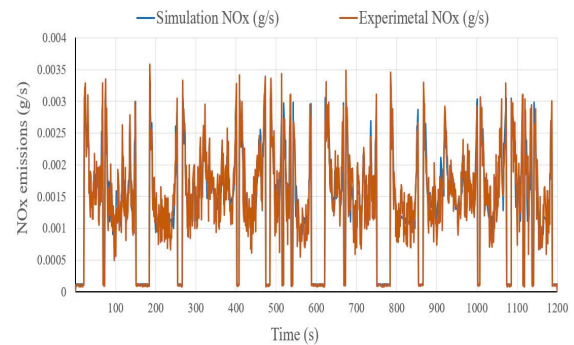


Fig. 11. NO_x emissions with WMTC cycle

Table 5. Comparison of the average emissions over WMTC cycle between simulated and measured results.

Emissions	Measured values	Simulated values	Difference
HC (g/km)	0,505	0,518	2,57 %
CO (g/km)	2,248	2,283	1,53 %
NO _x (g/km)	0,142	0,145	1,99 %

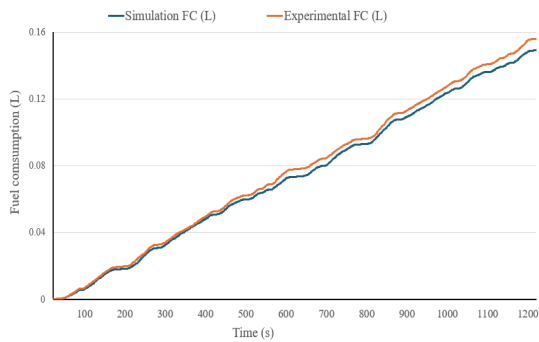


Fig. 12. Fuel consumption with WMTC cycle

Similarly, the model's fuel consumption was validated against experimental data (Fig. 12). The results showed that under the WMTC cycle, with an average driving speed of 28.92 km/h, the model consumed 0.15183 liters, equivalent to 1.575 liters per 100 km, differing by only 2.35% from the experimental value of 0.1554 liters, or 1.612 liters per 100 km. This small deviation further reinforces the reliability of the model in simulating not only emissions but also fuel consumption.

Through the above results, the motorcycle model is validated and possible to use for simulation work with other driving cycles such as ECE-R40 and HMDC cycles.

The simulation speeds of the ECE R40 and HMDC driving cycles are presented in Fig. 13 and Fig. 14 respectively.

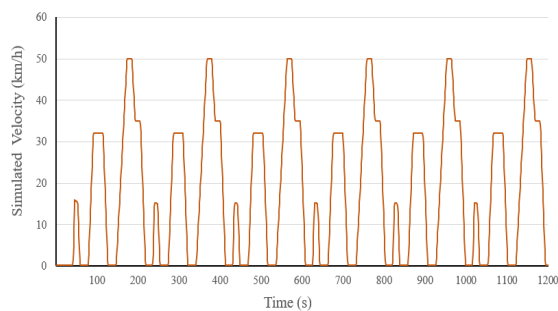


Fig. 13. Simulated velocity according to ECE R40 cycle

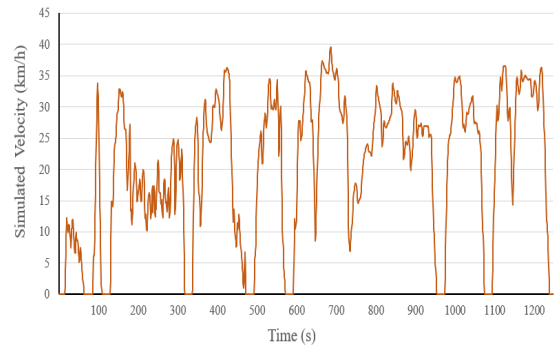


Fig. 14. Simulated velocity according to HMDC cycle

Emission simulation according to the ECE R40 and HMDC driving cycles is shown in Figs. 15 to Fig. 20.

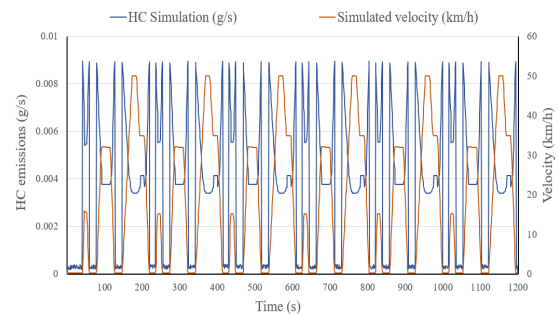


Fig. 15. HC emission flow chart according to ECE-R40 driving cycle

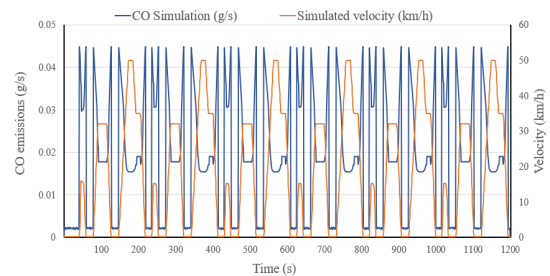


Fig. 16. CO emission flow chart according to ECE-R40 driving cycle

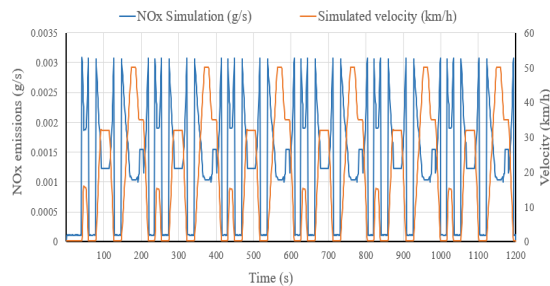


Fig. 17. NO_x emission flow chart according to ECE-R40 driving cycle

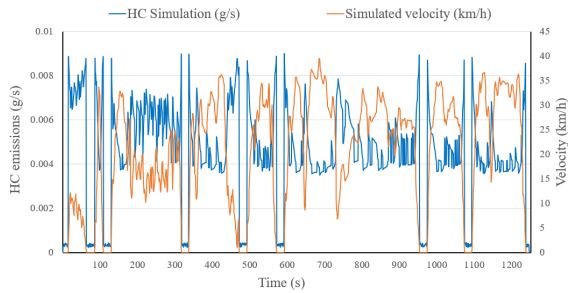


Fig. 18. HC emission flow chart according to HMDC driving cycle

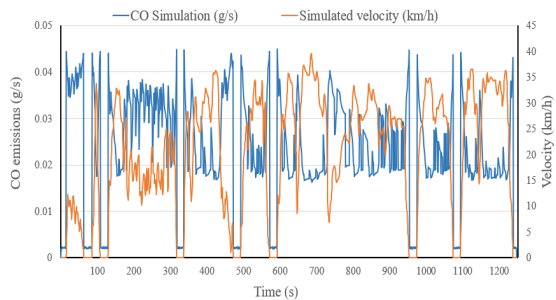


Fig. 19. CO emission flow chart according to HMDC driving cycle

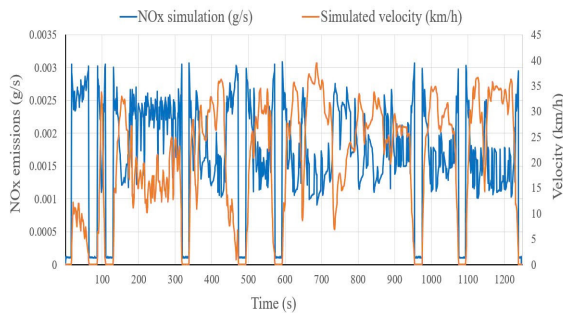


Fig. 20. NO_x emission flow chart according to HMDC driving cycle

Table 6. Average emissions when simulating two cycles HMDC and ECE R40

Emissions	HMDC	ECE R40	HMDC/ECE
HC (g/km)	0.572	0.575	0.994
CO (g/km)	2.018	2.447	0.824
NO _x (g/km)	0.151	0.159	0.949

Calculated over the entire cycle, the average emissions of Honda Future 125 Fi corresponding to the two HMDC and ECE R40 cycles are determined in the Table 6.

Table 6 shows that the average emission ratio between the two HMDC and ECE R40 cycles for the three emission components HC, CO, NO_x are 0.994; 0.824; 0.949 respectively. In general, the difference between the average emission results of the HMDC cycle and the ECE R40 cycle for the three parameters HC, CO, NO_x is not large, ranging from 0 to 2%. In addition, the average HC, CO, NO_x emissions of the HMDC driving cycle are lower than the ECE R40 driving cycle, which also shows that the engine combustion process is better.

Calculated over the entire cycle, the average emissions of the Honda Future 125 Fi corresponding to the cycles are given in Table 7.

The significant differences in average emissions of CO, HC, and NO_x across various driving cycles demonstrate that factors such as speed, operating conditions, and simulated traffic characteristics substantially influence emission outcomes. This finding underscores the critical importance of selecting an appropriate driving cycle to ensure the accuracy of emission simulations.

Subsequently, the authors compared the simulated emission results for HC, CO, and NO_x from 0 to 350 seconds, clearly illustrating the differences in emission flow rates across the three driving cycles: WMTC, HMDC, and ECE R40. The results are depicted from Fig. 21 to Fig. 23.

Table 7. Average emissions when simulating the cycles

Emissions	WMTC	ECE-R40	HMDC
HC (g/km)	0.518	0.575	0.572
CO (g/km)	2.283	2.447	2.018
NO _x (g/km)	0.145	0.159	0.151

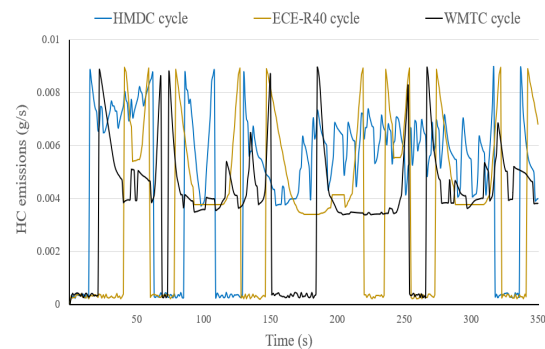


Fig. 21. HC emissions according to 3 driving cycles

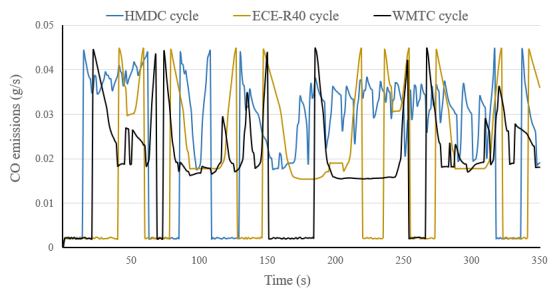


Fig. 22. CO emissions according to 3 driving cycles

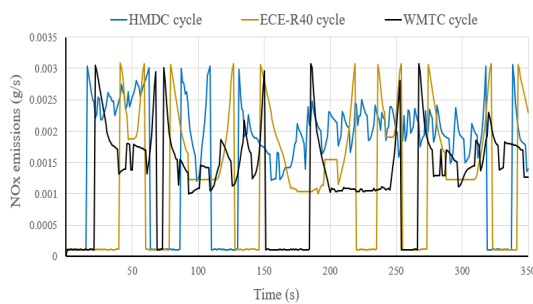


Fig. 23. NO_x emissions according to 3 driving cycles

Among the three driving cycles, HMDC stands out with continuous oscillations, reflecting the rapid fluctuations in emission levels under urban traffic conditions in Vietnam, characterized by frequent acceleration, sudden braking, and short waiting periods. In contrast, WMTC exhibits less pronounced oscillations compared to HMDC but still captures emission variations across different operating states, representing a mix of urban traffic and suburban or highway segments. Meanwhile, ECE R40 demonstrates smoother oscillations with minimal sharp fluctuations, primarily simulating stable traffic conditions and lacking the complexity of modern traffic environments.

These characteristics highlight the differences in each cycle's ability to reflect real-world traffic conditions and emphasize the suitability of HMDC cycle for evaluating emissions in Vietnam. Therefore, in the absence of a specific driving cycle for motorcycles in Vietnam, HMDC emerges as a more appropriate choice for simulating emissions under the country's actual traffic conditions.

5. Conclusion

The research results demonstrate that each driving cycle has a distinct impact on CO, HC, and NO_x emissions, with significant variations observed across the cycles. The HMDC, which effectively captures Vietnam's typical traffic scenarios, has been identified as a suitable choice for simulating motorcycle emissions under urban traffic conditions in

the country. These findings not only support emission estimation efforts but also contribute to the development of air pollution control strategies, paving the way for a more sustainable transportation environment in the future.

Although the study focuses on a specific motorcycle model and three driving cycles, it highlights the potential of simulation methods in reducing testing costs and supporting the development of more effective pollution control strategies. Future research could expand the model to incorporate real-world driving data and apply it to a broader range of motorcycle types to enhance generalizability. Furthermore, integrating advanced emission control technologies into the model could significantly improve its accuracy and applicability.

Acknowledgements

The authors would like to thank AVL Company (Austria) for providing the AVL Cruise M software for this study.

References

- [1] Jin Y., Andersson H., Zhang S., Air pollution control policies in China: A retrospective and prospects, *Int. J. Environ. Res. Public Health*, vol. 13, iss. 12, Dec. 2016. <https://doi.org/10.3390/ijerph13121219>
- [2] Linh Thy Le, Khanh Bang V. Quang, Trieu Vi Vo *et al*, 2024, Environmental and health impacts of air pollution: a mini review, *Environmental Sciences*, vol. 66, no. 1, Mar. 2024. [https://doi.org/10.31276/VJSTE.66\(1\).120-128](https://doi.org/10.31276/VJSTE.66(1).120-128)
- [3] Hien Tran, Trung Dung Nghiem, Khue Ngoc Hoang Vu and Bang Quoc Ho, Characteristics and distribution of greenhouse gas emissions from motorcycles in Hanoi, Vietnam, *IOP Conference Series: Earth and Environmental Science*, vol. 1349, Oct. 2023. <https://doi.org/10.1088/1755-1315/1349/1/012040>
- [4] Kawamoto R., Mochizuki H., Moriguchi Y., Nakano T., Motohashi M., Sakai Y., Inaba A., Estimation of CO₂ emissions of internal combustion engine vehicle and battery electric vehicle using LCA, *Sustainability*, vol. 11, iss. 9, May. 2019. <https://doi.org/10.3390/su11092690>
- [5] Hu H, Lee G, Kim J.H, Shin H, Estimating micro-level on-road vehicle emissions using the K-means clustering method with GPS big data, *Electronics*, vol. 9, iss. 12, Dec. 2020. <https://doi.org/10.3390/electronics9122151>
- [6] Obaid M., Torok A., Ortega J., A comprehensive emissions model combining autonomous vehicles with park and ride and electric vehicle transportation policies, *Sustainability*, vol. 13, iss. 9, Apr. 2021. <https://doi.org/10.3390/su13094653>
- [7] Hatzopoulou M., Miller E. J., Santos B., Integrating vehicle emission modeling with activity-based travel

- demand modeling: case study of the Greater Toronto, Canada, Area, Transportation Research Record: Journal of the Transportation Research Board, vol. 2011, iss. 11, Jan. 2007.
<https://doi.org/10.3141/2011-04>
- [8] Al-Turki M., Jamal A., Al-Ahmadi H. M., Al-Sughaiyer M. A., Zahid M., On the potential impacts of smart traffic control for delay, fuel energy consumption, and emissions: an NSGA-II-based optimization case study from Dhahran, Saudi Arabia, Sustainability, vol. 12, iss. 18, Sep. 2020.
<https://doi.org/10.3390/su12187394>
- [9] S. A. Evangelou and W. Shabbir, Dynamic modeling platform for series hybrid electric vehicles, IFAC-PapersOnLine, vol. 49, iss. 11, pp. 533–540, Jun. 2016.
<https://doi.org/10.1016/j.ifacol.2016.08.078>
- [10] Bessagnet, B.; Allemand, N.; Putaud, J.P.; Couvidat, F.; André, J.M.; Simpson, D.; Pisoni, E.; Murphy, B.N.; Thunis, P., Emissions of carbonaceous particulate matter and ultrafine particles from vehicles - a scientific review in a cross-cutting context of air pollution and climate change, Applied Sciences, vol. 12, iss. 7, Apr. 2022.
<https://doi.org/10.3390/app12073623>
- [11] H. D. Tung, H. Y. Tong, W. T. Hung, N. T. N. Anh, Development of emission factors and emission inventories for motorcycles and light duty vehicles in the urban region in Vietnam, Science of the Total Environment, vol. 409, iss. 14, pp. 2761-2767, Jun. 2011.
<https://doi.org/10.1016/j.scitotenv.2011.04.013>
- [12] Yen-Lien T. Nguyen, Trung-Dung Nghiem, Anh-Tuan Le, Khanh Nguyen Duc, Duy-Hung Nguyen, Emission characterization and co-benefits of bus rapid transit: a case study in Hanoi, Vietnam, Atmospheric Pollution Research, vol. 12, iss. 8, Aug. 2021.
<https://doi.org/10.1016/j.apr.2021.101148>
- [13] Duc, K. N., Nguyen, Y.-L. T., Duy, T. N., Le, A.-T., Huu, T. P., A robust method for collecting and processing the on-road instantaneous data of fuel consumption and speed for motorcycles, Journal of the Air and Waste Management Association, vol. 71, iss. 1, pp. 81–101, Nov. 2020.
<https://doi.org/10.1080/10962247.2020.1834470>
- [14] Nguyen Huu Can, Du Quoc Thinh, Pham Minh Thai, Nguyen Van Tai, Le Thi Vang, Theory of Tractors, Scientific and Technical Publishing House, pp. 22-35, 2007.
- [15] Onorati A., Ferrari G., D'Errico G., 1D unsteady flows with chemical reactions in the exhaust duct-system of S.I. engines: predictions and experiments, SAE Technical Paper 2001-01-0939.
<https://doi.org/10.4271/2001-01-0939>
- [16] Onorati A., Ferrari G., D'Errico G., 1D unsteady flows with chemical reactions in the exhaust duct-system of S.I. Engines: predictions and experiments, SAE Paper, Mar. 2001.
<https://doi.org/10.4271/2001-01-0939>
- [17] D' Errico G., Ferrari G., Onorat A. and Cerri T., Modeling the pollutant emissions from a S.I. engine, SAE Paper, Mar. 2002.
<https://doi.org/10.4271/2002-01-0006>
- [18] Lavoie G. and Blumberg P. N., A fundamental model for predicting consumption, NO_x, and HC emissions of the conventional spark-ignition engines, Combustion Science and Technology, vol. 21, iss. 5-6, pp. 225-258, 1980.
<https://doi.org/10.1080/00102208008946939>